JOINT EUROPEAN TORUS JET

JET–P(92)89

A. Gondhalekar, P.C. Stangeby, J.D. Elder
and JET Team

Investigations of Impurity Control in JET using Fueling, and Interpretation of Experiments using the LIM Impurity Code

Investigations of Impurity Control in JET using Fueling, and Interpretation of Experiments using the LIM Impurity Code

A. Gondhalekar, P.C. Stangeby[1], J.D. Elder[1] and JET Team*

JET-Joint Undertaking, Culham Science Centre, OX14 3DB, Abingdon, UK

[1]Institute for Aerospace Studies, University of Toronto, Canada
** See Annex*

Preprint of Paper to be submitted for publication in
Nuclear Fusion

Investigations of Impurity Control in JET using Fueling, and Interpretation of Experiments using the LIM Impurity Code

A.Gondhalekar, P.C.Stangeby[+] and J.D.Elder[+]

JET Joint Undertaking, Abingdon, OX14 3EA, United Kingdom
and [+]Institute for Aerospace Studies, University of Toronto, Canada

ABSTRACT

Inhibition of contamination of the plasma core in JET by edge impurities during high power heating of deuterium plasmas in limiter configuration using fueling is demonstrated. By injecting deuterium gas during heating, in the presence of very much larger recycling deuterium flux, a reduction of more than factor two was effected in $n_z(0)/\Phi_z$, the ratio of central impurity density to impurity influx at the plasma edge. The reduction in $n_z(0)$ was obtained without much effect on peak electron temperature and density. Reduction of plasma contamination by gas fueling was observed also when hot spots formed on the limiter, a condition that without simultaneous gas fueling culminated in runaway plasma contamination.

Detailed analysis of the experiments is undertaken with the purpose of identifying the processes by which plasma contamination was inhibited, employing standard limiter plasma contamination modeling. Processes which might produce the observed impurity inhibiting effects of gas injection include (a) reduction in impurity production at the limiter, (b) increase in impurity screening in the scrape-off layer, (c) increase in radial impurity transport at the plasma edge, (d) increase in average deuteron flow velocity to the limiter along the scrape-off layer. These are examined in detail using the Monte Carlo limiter impurity transport code LIM. Bearing in mind that uncertainties exist both in the choice of appropriate modeling assumptions to be used and also in measurement of required edge plasma parameters, impurity modeling of changes in $n_z(0)/\Phi_z$ by factor two is at the limit of present capability. However, comparison between LIM code simulations and measurements of plasma impurity content indicate that the standard limiter plasma contamination model may not be adequate and that other processes need to be added in order to be able to describe the experiments in JET.

1. Introduction

The increase in Z_{eff} of deuterium plasmas in JET in limiter configuration during high power Ion Cyclotron Resonance Frequency(ICRF) and Neutral Beam Injection(NBI) heating may be attributed to greater impurity influx due to increase in edge plasma temperature and density. Experiments to inhibit this increase in Z_{eff} by deuterium gas injection during heating are reported. A prerequisite for such explorations is that recycling be reduced so that plasma density control is maintained during fueling. This requirement is met in beryllium limiter and beryllium gettered carbon limiter operation in JET during which pumping of deuterium is observed.

Fuel gas injection is simple and is found to be consistently successful in inhibiting impurity increase in the plasma core during high power heating. No doubt the amount of gas injected can be made so large that a reduction in Z_{eff} is effected by dilution, while the overall plasma reactivity is degraded due to lower temperature. This is not the aim of these experiments. It is to enrich the fuel without increasing $\bar{n}_e$ or reducing $T_i(0)$ or degrading fusion reaction rate.

2. Experiments to reduce plasma contamination by gas fueling

Experiments were performed in deuterium plasmas in toroidal belt-limiter configuration, in beryllium gettered carbon limiter(C-L) and beryllium limiter(Be-L) operations. A detailed account of the experiments has been given earlier[1]. For illustration of the simulations two specimen target plasmas are discussed here, with the following parameters:

C-L operation in which carbon was the main impurity, with B_ϕ=3.2T, I_ϕ= 3MA, $\bar{n}_e \cong 4.5\times10^{19}m^{-3}$, $T_e(0)\cong$8.6keV, and $Z_{eff}\cong$4, with P_{NBI}=5.3MW and P_{ICRF}=8.8MW.

Be-L operation in which beryllium was the main impurity, with B_ϕ=2.1T, I_ϕ=3MA, $\bar{n}_e\cong4.5\times10^{19}m^{-3}$, $T_e(0)\cong$6.5keV, and $Z_{eff}\cong$2.5, with $P_{NBI}\cong$8MW and $P_{ICRF}\cong$8MW.

Fig.1 compares evolution of $\bar{n}_e$ and Z_{eff} for two discharges in the C-L operation. The two discharges were identical in all respects except that one was without(#19643) and the other with(#19648) gas injection during ICRF heating, at a rate of ≅57 mbl/s. The amount of gas injected was adjusted so that the increase in $\bar{n}_e$ and reduction in $T_e(0)$ due to the gas pulse were minimized. The recycling deuteron flux in #19643 corresponded

to ≅ 3.7 bl/s. Fig.1 shows that injecting a tiny amount of additional gas during ICRF heating effected a large reduction in Z_{eff}. Similar results were obtained also in the Be-L operation. We attribute the reduction in Z_{eff} to reduction of impurity density in the plasma core.

Fig.2 illustrates the effect of gas injection on evolution of peak electron, deuteron, and the carbon densities, $n_e(0)$, $n_D(0)$, and $n_C(0)$ respectively, for the C-L operation. Evolution of $n_D(0)$ and $n_C(0)$ were inferred from measurements of spatial profiles of visible bremsstrahlung (VB)[2], from which the Z_{eff} shown in fig.1 was obtained. A mixture of principal impurities was assumed, $n_C:n_{Be}=5:1$, inferred from spectroscopic measurements. For comparison and validation, $n_C(0)$ was also deduced from absolute measurements of spatial profile of soft x-ray bremsstrahlung emission(SXR), using the same impurity mix as for the VB. $n_C(0)$ was also directly measured using charge-exchange recombination spectroscopy (CXRS) [3]. **Table I** summarizes measurements for a pair of shots on carbon limiters. Although the three measurements of $n_Z(0)$ differ in absolute magnitude, they all give the same relative reduction of $n_Z(0)$ when gas was injected. Also tabulated are corresponding edge plasma parameters, inferred from Langmuir probe measurements, which will be used for analysis and interpretation of these experiments.

Thus by injecting D_2 at the plasma edge during high power ICRF heating a reduction in absolute $n_C(0)$ by ≅1.7 and an increase in $n_D(0)/n_e(0)$ by ≅1.7 was effected, while $n_e(0)$ increased by ≤1.05 and $T_e(0)$ decreased by ≅0.85. **Table I** shows that a similar result was obtained also for the Be-L operation where $n_{Be}(0)$ was deduced as before from VB, using $n_{Be}:n_C=40:1$. $n_{Be}(0)$ was measured also by CXRS. Once again when a small amount of D_2 gas was injected during heating, a reduction in $n_{Be}(0)$ by ≅2 and an increase in $n_D(0)/n_e(0)$ by ≅1.3 was observed, while increasing $n_e(0)$ by ≤1.05 and reducing $T_e(0)$ by ≅0.85.

Further experiments with beryllium limiters using higher power heating showed that sometimes hot spots formed on the limiters, giving runaway contamination of the plasma. This was attributed to overheating of edges of limiter tiles culminating in evaporation and melting, giving a large beryllium impurity source. Contamination of the plasma was inhibited by injecting deuterium gas at the same time as the high power heating. A

summary of the observations is shown in **Table II**. An Ohmically heated specimen deuterium plasma (#22948), with I_ϕ=3MA, was sustained by deuterium and beryllium influxes Φ_D and Φ_{Be}, measured using D_α(6561Å) and BeII(4361Å) emissions, giving Z_{eff}=1.5. This plasma was then further heated with NBI and ICRF power, causing hot spots to form whereby the beryllium influx and Z_{eff} increased by a large amount. This level of contamination could be sustained for ≤1.5s, during which time Φ_{Be} continuously increased and the D-D reaction rate R_{DD} rapidly declined to insignificance due to dilution of the deuterium fuel.

When deuterium gas was injected during ICRF heating and with a hot spot present, #22957, a high D-D reaction rate could be sustained for many seconds. Although Φ_{Be} increased by a factor ≥10 compared to that in #22948 during ICRF heating, runaway contamination was arrested without reducing R_{DD}. **Table II** summarizes observations of #22948 and #22957 during Ohmic and additional heating, with and without gas injection.

This method for reducing central impurity density is a valuable advance, and because of its simplicity, small cost and effectiveness, it has been exploited widely during high power heating in JET, in limiter and X-point configurations. This method is likely to attract increased application and it is therefore worth while to find out how it works and how to make it more effective.

3. Simulation of observed impurity shielding effects

The standard model for limiter impurity behaviour is described in its basic form by Engelhardt and Feneberg[4]. In the following we examine in detail simple well known processes which could supposedly give the observed impurity reduction due to external gas fueling. The different hypothesis are:

a. Additional fueling cools the edge plasma so that the impurity production rate is reduced and the new steady state impurity density in the plasma core corresponds to a smaller source.

b. Increased fueling changes the edge density and temperature such that the impurities are ionized at a larger radius, more effectively retained in the SOL and thus better screened from the bulk plasma.

c. Additional fueling modifies edge transport and increases the cross-field impurity ion outflux, inhibiting impurity penetration to the plasma core.

d. Additional fueling changes the flow pattern of the background deuterium plasma along the scrape-off layer(SOL), changing the strength of the sink action of the SOL for impurities.

We present simulations of experiments described earlier, using a model of limiter plasma contamination incorporating the above hypothesis, and go on to demonstrate the inadequacy of the processes listed above alone to reproduce the experimentally observed impurity behavior.

In (d) the frictional force which drags impurity ions to the limiters, the sink in this system, is usually the most important force for removing impurities from the plasma. The changes mentioned in (d) could also be described as an edge screening effect, but a distinction is made here between this effect and those in (b) and (c).

The potential for the above effects to give the observed results is examined using a 2-D Monte Carlo impurity simulation code LIM (Limiter Impurity), which is briefly described in the next section. A preliminary account of this work was given earlier[1,5]. The core impurity level is a result of a chain of processes, and each step contributes non-negligible errors and uncertainties, making reliable simulation of central impurity level to within a factor two at the limit of present ability. This caveat is discussed in greater detail later but is noted here to emphasize that conclusions from this type of undertaking must be applied with caution.

Next, the LIM code used in the present work is described. An analytic model of impurity behavior is described in the following section. In subsequent sections simulations are performed for pairs of JET pulses free from hot spots on the limiters, with and without gas injection. The next section gives results for JET pulses on Be-limiters with hot spots, but without additional fuel gas injection, followed by a section on pulses on Be-limiters with hot spots and employing additional gas fueling. The paper concludes with sections on uncertainties and errors.

4. The LIM impurity transport code

An initial and substantial reduction in uncertainties in simulation of plasma contamination can be achieved by reducing to a minimum the use of derived quantities and relying as far as possible on measured data for input to modelling. It is very valuable when the plasma background, in the form of radial profiles of electron temperature and density, $T_e(r)$ and $n_e(r)$, is known from measurements for input to the simulation. $T_i(r)$, and $Z_{eff}(r)$ are also required for input but often not available. Usually $T_e=T_i$ is assumed. In such an interpretive approach, as distinct from a predictive one, important processes such as feedback on the main plasma constituents of evolution of impurities, such as changes in T_e due to impurity radiation, are effectively included. Also, by eliminating the need to simulate behavior of the main plasma constituents, complexity in modeling of impurity behavior can be tolerated, e.g. finite impurity ion thermalization rates can be followed.

The LIM code has been described elsewhere[5,6] and will only be briefly outlined here. It has been developed in the spirit of the Monte Carlo impurity code work of Brooks[7] and early work by Sengoku[8]. The plasma background is input in the form of measurements of profiles of T_e, T_i and n_e. Quantities which were not accessible to measurement, such as deuteron drift velocity and electrostatic field in the SOL, v_{D+} and E_{SOL}, together with their radial and toroidal variations, are input from separate model calculations. Measured Z_{eff} can be input so that collisionality is taken properly into account, although it is also calculated. The limiter and magnetic configurations are specified. Spatial and energy distributions of the D+ flux to the limiter are then calculated and, thus also, the spatial distribution of sputtering and sublimation products. Individual neutrals are then launched in a Monte Carlo way, weighted by the spatial distribution of production and with an energy drawn from the Thompson distribution[9], and an angle to the local surface drawn from a cosine distribution. Physical sputtering yields are taken from Bohdansky formulae[10] with Roth's adjustments[11]. The maximum sputtered neutral energy is cut-off as appropriate for D+ or for self-sputtering[10]. For the most part it is assumed here that normal incidence ion yields apply, even though the actual angle of ion incidence to the surface can be

glancing. While for highly polished crystalline surfaces the yield can be greatly enhanced at oblique incident angles [12,13], for technical grade surfaces the enhancement is small. The ions are then followed throughout the plasma until they return to the limiter where the self-consistent self-sputtering is calculated.

5. A simple limiter plasma contamination model

The chain connecting the edge impurity source to central impurity density consists of three major links: production, edge screening/transport, and core transport. In steady-state, with toroidally and poloidally uniform influx of impurity neutrals and outflux of impurity ions, it can be shown [1,14,15] that the central impurity density $n_z(0)$ is given by

$$n_z(0) = \frac{(\lambda^0_{iz}+\lambda_{SOL})\phi^0_z \exp(f)}{A_P D_z} \qquad \text{eq.1}$$

λ^0_{iz} is the depth inboard of the last closed flux surface(LCFS) at which neutrals are ionized, $\lambda^0_{iz} = |v^0_z|/n_e\langle\sigma v\rangle$, where $|v^0_z|$ is average velocity of incident impurity neutrals. λ_{SOL} is radial length scale for impurity density decay in the SOL, $\lambda_{SOL}=(D_z\tau_{SOL})^{1/2}$ where τ_{SOL} is the dwell time of impurities in the SOL and D_z is cross-field impurity density diffusivity. f is a scaling factor corresponding to an assumed form of core impurity transport where the convection(pinch) velocity is written as $v_z = -2fD_z r/a^2$, where r is the minor radial coordinate and a is the minor radius of the LCFS. Generally $f\approx 1$ is deduced for the core. ϕ^0_z is the rate of impurity atom production at the plasma edge, which is enclosed by a surface of area A_P.

The average impurity density $\bar{n}_z$ is given by an expression like eq.1 where exp(f) is replaced by g where

$$g = [\exp(f)-1]/f \qquad \text{eq.2}$$

Eq.1 illustrates the main links connecting ϕ^0_z and $n_z(0)$, showing that:

a. $n_z(0)$ is proportional to the impurity production rate ϕ^0_z.

b. The dependence of $n_z(0)$ on edge transport and screening is controlled through $(\lambda^0_{iz}+\lambda_{SOL})$. The deeper the neutrals penetrate the plasma before being ionized, larger λ^0_{iz}, the larger is $n_z(0)$. The longer the ions spend in the SOL, i.e. weaker the sink action of the SOL, the larger is τ_{SOL}, λ_{SOL} and therefore $n_z(0)$.

c. The dependence of $n_z(0)$ on core transport is given by the factor exp(f) for the assumed relation between D_z and v_z.

From the above it follows that in a cylindrical plasma of radius a, the impurity confinement time, defined as $\tau_z=\int n_z(r)dV/\phi^0_z$, is given by

$$\tau_z=a(\lambda^0_{iz}+\lambda_{SOL})g/2D_z \qquad \text{eq.3}$$

τ_z is independent of ϕ^0_z and thus its magnitude is a measure of transport alone. For limiter plasmas the convective term v_z is generally effective only over large distances O(a); it can often be neglected in the edge region, $a-\lambda^0_{iz}<r<a+\lambda_{SOL}$. Thus if f is set to zero then τ_z gives a measure of edge transport and screening alone.

From the foregoing and as noted earlier we see that there are four ways in which a reduction in core impurity density $n_z(0)$ could come about due to increased fueling, according to this standard contamination model. These are:

a. Reduction in impurity production, thus reducing influx ϕ^0_z.

b. Increase in impurity screening due to changes in edge conditions, giving a reduction in λ^0_{iz}, τ_{SOL} and λ_{SOL}. An increase in edge T_e and n_e would reduce λ^0_{iz}. τ_{SOL} would reduce because ions created closer to the LCFS (smaller λ^0_{iz}) would radially diffuse into the SOL closer to the limiter.

c. Changes of radial transport could affect core transport through the term exp(f), and also edge transport through D_z and $(D_z\tau_{SOL})^{1/2}$ terms. In the simple model, changing core and edge transport separately would require changing f and D_z separately since D_z is assumed to be spatially constant. In the LIM code, D_z can be varied spatially and the effect of edge vs. core transport changes can be investigated in that way, as well as via changes in f.

d. Changes in the plasma flow pattern in the SOL would change the impurity dwell time τ_{SOL}.

While the LIM code does not use either eq.1 or eq.2, or the simplifying assumptions underlying these expressions, these relations illustrate the different links between $n_z(0)$ and ϕ_z^0. They also show the sensitivity of $n_z(0)$ to the different factors which play a role; for example, that the effect of changes in λ_{iz}^0 or λ_{SOL} separately are diluted because the sum $(\lambda_{iz}^0+\lambda_{SOL})$ is involved. These expressions serve also in making first order consistency checks for the code calculations. The code separately calculates $n_z(0)$, $\bar{n}_z$ and τ_z, and these quantities are required to satisfy the condition $\bar{n}_z V_p \approx \phi_z^0 \tau_z$, where V_p is the plasma volume. The average depth at which ionization takes place, $\bar{\lambda}_{iz}^0$, and the average dwell time in the SOL, $\bar{\tau}_{SOL}$, are also calculated. The latter can be inserted in eq.1 and eq.3 to test for internal consistency of the code output. The checks are only first order since uniformity of influx and outflux are assumed in applying eq.1 and eq.3. whereas the code calculation is free of these.

6. Simulations of matched pairs of shots

Table I summarizes measurements of central impurity density and Langmuir probe measurements of edge plasma conditions. Beryllium gettering of the walls effectively eliminated oxygen contamination. These discharges are thus particularly interesting for analysis because there is virtually only one impurity species present.

The LIM code simulations used the measured $T_e(r)$, $n_e(r)$ profiles and assumed $T_e = T_i$. Physical sputtering by deuterium plus self-consistent self-sputtering with normal incidence ion yields were used. For most of the analysis $D_z=0.54$ m^2/s and $v_z = -2D_z r/a^2$ were used, based on earlier analysis of electron density transport[16], assuming that the same transport coefficients apply to impurities.

The sink action of the SOL on impurities depends on the magnitude and spatial variation of the plasma flow speed in the SOL v_{D+}, and electric field in the SOL E_{SOL}, both along the magnetic field, quantities for which there are virtually no measurements in any tokamak, but only model results. For example, a simple 1-D fluid model[17] with uniform source along the SOL tube length, due to cross-field transport across the LCFS from the confined plasma, gives a nonlinear spatial variation of $v_{D+}(y)$ and $E_{SOL}(y)$, where y is measured along the SOL. Other models give other

y-variations[18]. Virtually all models assume that $v_{D+} \rightarrow c_s$ at the limiter sheath, where the ion acoustic speed $c_s = \sqrt{[k(\gamma T_D + T_e)/m_D]}$. For impurities the frictional force associated with v_{D+} is usually more important than the electrostatic forces or temperature gradient forces [15,6]. For the LIM simulations a simple linear dependence on coordinate y was in general employed for $v_{D+}(y)$ and $E_{SOL}(y)$, with $v_{D+}=c_s$ and $E_{SOL} = -kT_e/2L$ at the limiter, where the connection length is taken to be L=40m.

In the simulations the non-circular toroidal geometry of the JET plasma was employed. An assumption was made that the two toroidal belt limiters were uniformly loaded, giving four plasma-wetted surfaces, an assumption that could not be verified. Thus if the limiters were not equally loaded there is the possibility that the calculated absolute influx ϕ_z^0 and impurity density $n_z(0)$ are overestimated by up to factor ≅2. However, provided fuel gas injection did not modify limiter power distribution, the relative comparisons of ϕ_z^0 and $n_z(0)$ would remain unaffected.

6.1 Change in impurity production rate

As can be seen from **Table I**, gas injection significantly increased the edge density without greatly reducing the edge temperature, suggesting an *increase* in impurity production rather than a reduction. The simulations, **Table III**, confirmed an increase in ϕ_z^0 due to gas injection. The observed reduction in $n_z(0)$ therefore implies that whatever process caused this, it had to do so in spite of an increase in impurity production. Note that absolute values ϕ_z^0 in **Table III** have been corrected by a constant factor relative to the earlier tabulations[5] to allow for total production at the limiters.

Impurity confinement time τ_z and central impurity density $n_z(0)$, computed independently in the LIM code, are given in **Table III**, showing that gas injection reduces τ_z thereby contributing to reduction of $n_z(0)$. This contribution is canceled by an increase in influx ϕ_z^0, giving the net effect that the measured reduction in $n_z(0)$ of a factor ≅2 can not be simulated this way. Also shown in **Table III** are the simulated average charge $\bar{Z}_{lim}$ of the ion mixture striking the limiter. Due to shorter $\bar{\tau}_{SOL}$ and τ_z, $\bar{Z}_{lim}$ is reduced slightly during gas injection.

Table IV gives further details of LIM simulation of impurity production. The deuteron flux ϕ_{D+} was calculated by assuming

$$\phi_{D+}=4\cdot(2\pi R_L)n_e(a)c_s(a)\sin\theta_B\lambda_\Gamma \qquad \text{eq.4}$$

The factor 4 is the number of wetted surfaces, R_L=4m is the major radius of the belt limiter, $n_e(a)=n_{LCFS}$ and $c_s(a)$ are the electron density and acoustic speed respectively at the LCFS, and θ_B is the pitch angle of the magnetic field at the limiter, taken to be a fixed 15° here. λ_Γ is the scrape-off length for the particle flux, $\lambda_\Gamma=[\lambda_n^{-1}+(2\lambda_T)^{-1}]^{-1}$. Then $\phi_Z^0=Y_{TOT}\phi_{D+}$ where Y_{TOT} is the total sputtering yield, including self-sputtering. Particle flux density at the LCFS is taken to be $n_e(a)\cdot c_s(a)$, although probably it should be $\approx 1/2\cdot n_e(a)\cdot c_s(a)$ [18], thus making the calculated ϕ_Z^0 and $n_Z(0)$ too large by a factor ≈2. ϕ_{D+} and ϕ_Z^0 are given in **Table IV**. Notice that although, as expected, the yields are not much affected by gas injection, impurity production increased due to greater deuteron flux.

Simulations for the average ionization depth of neutrals inside the LCFS $\bar{\lambda}_{iz}^0$, and the average dwell-time of impurity ions in the SOL $\bar{\tau}_{SOL}$, are given in **Table III**, along with $\lambda_{SOL}=(D_Z\bar{\tau}_{SOL})^{1/2}$. These can be inserted into eq.1 and eq.3 to perform a first order consistency check of $n_Z(0)$ and τ_Z. If $\bar{\lambda}_{iz}^0$ were large, then even if ϕ_Z^0 were toroidally/poloidally localized, eq.1 and eq.3 would be expected to be good approximations since the ions would rapidly spread themselves uniformly around the torus before undergoing much cross-field transport, making the effective influx and outflux uniform. However, for the present cases $\bar{\lambda}_{iz}^0$ is only a few mm. It may seem surprising therefore that eq.1 and eq.3 give close agreement with directly calculated values of $n_Z(0)$ and τ_Z shown in **Table V**, as if in using the simulated values of $\bar{\tau}_{SOL}$ and λ_{SOL} nonuniformity in source and sink was taken into account. Similar close agreement between the two approaches has been obtained in a wide range of other LIM simulation studies, the agreement breaking down only when $\bar{\lambda}_{iz}^0<0$, meaning that ionization takes place well outside the LCFS. Eq.1 is modified when $\lambda_{iz}^0<0$ and the term $(\lambda_{iz}^0+\lambda_{SOL})$ is then replaced by $\lambda_{SOL}\exp(\lambda_{iz}^0/\lambda_{SOL})$ [14]. A significant discrepancy with the directly calculated values of $n_Z(0)$ nevertheless arises when $\lambda_{iz}^0 \ll 0$. The computational effort required to obtain $\bar{\tau}_{SOL}$ or $n_Z(0)$ directly is the same. One also needs to compute $\bar{\lambda}_{iz}^0$,

although that usually requires relatively little computational time. 10^4 primary sputtered neutrals, plus associated secondaries, tertiaries, etc. were launched to obtain the results of **Tables III-V**. Time steps of 10^{-8}s for neutrals and $3x10^{-7}$s for ions were employed, requiring 15-20 minutes of computational time on a CRAY-XMP per case. The neutral part of the calculation required only 30-100 sec per case.

A second type of consistency check is that $\bar{n}_z V_p \approx \phi_z^0 \tau_z$ should hold, where V_p is the plasma volume (R_o=3m, a=1.15m, k=b/a=1.45, $V_p \cong 114m^3$). Values of $\bar{n}_z V_p / \phi_z^0 \tau_z$ given in **Table V** are close to one but not exactly unity, the scatter arising due to Monte Carlo nature of the calculation. The trend to lie below unity is attributed to the approximate way the non-circular toroidal shape of the plasma is treated; the code assumes a circular cylindrical plasma shape and computes n_z normalized to one neutral injected per sec per m^2 of plasma surface area. For the tabulated values of $n_z(0)$ one then multiplies this normalized value by ϕ_z^0/A_p where A_p is the surface area of the JET plasma, $A_p \cong 165m^2$.

To conclude this section, it is reiterated that a reduction of impurity production due to gas injection is ruled out as a cause for the observed reduction in $n_z(0)$. In fact the impurity source increases.

6.2 Edge impurity shielding(without change of transport)

We note from eq.1 that reduction in $(\lambda_{iz}^0 + \lambda_{SOL})$ will reduce $n_z(0)$. We call this impurity shielding, in contrast to impurity reduction by increased edge transport. From **Table III** we see that the changes in edge plasma caused by gas injection do, in fact, reduce both λ_{iz}^0 and λ_{SOL}, giving greater impurity shielding and a reduction in τ_z. **Table V** shows that also quantitatively these reductions in $\bar{\lambda}_{iz}^0$ and λ_{SOL} fit with the calculated reduction τ_z. But the increase in impurity source ϕ_z^0 offsets the improved shielding. Consequently, gas injection is calculated to have nearly no effect on impurity level, leaving $n_z(0)$ unchanged, as seen in **Table III**.

Note that $T_i = T_e$ is assumed in the plasma edge. It is possible that gas injection causes a greater reduction in T_i than that inferred from the measured reduction in T_e, causing a greater reduction in $(\lambda_{iz}^0 + \lambda_{SOL})$ and $n_z(0)$ than that deduced above. This however seems improbable since the gas injection amounts to only 5-10% of the total deuterium influx.

In conclusion, increase in edge shielding is also ruled out as the cause of the reduction in $n_z(0)$ observed in the experiment.

6.3 Change in transport

It is trivially clear from eq.1 that increasing D_z and/or decreasing the pinch term f will reduce $n_z(0)$. The degree of sensitivity is indicated by eq.1, and the LIM simulations confirmed this dependence. When D_z was doubled the calculated value of $n_z(0)$ was reduced by about a factor two. It was not necessary to change D_z throughout the plasma; doubling D_z only in a narrow shell $(a-2.5) \leq r(cm) \leq a$ reduced $n_z(0)$ by a factor of $\cong 2$, since it is only in the region where the neutrals are ionized that the value of D_z is important. Thus, local increase in impurity density diffusivity in the plasma edge would be sufficient to produce the observed reduction in $n_z(0)$. Whether or not such reduction occurs must be determined by measurement of impurity transport near the plasma edge for matching pulses, with and without gas injection.

Previous experiments have shown that in JET impurity and electron density transport can be described by the same form of particle flux and with the same coefficients. Using this fact, one can test for the possibility of changes in D_z or v_z for impurities over longer spatial scale lengths since such changes should manifest themselves in modifications of the electron density profile $n_e(r)$, assuming that gas injection modifies transport of electron density in the same way as that of impurities. This possibility was tested and measurements of the electron density profile $n_e(r)$ did not support this hypothesis[2]. Impurity transport was measured directly using the laser blow-off method[19], but again no evidence was found to support the notion that gas injection increased D_z. It is more difficult to test the hypothesis of changed transport just at the edge. It is probable that such changes would influence the SOL as well as the impurity ionization region just inside the LCFS, making it difficult to separate the effects.

In conclusion, while modifications of impurity transport could certainly simulate the observed reduction in $n_z(0)$, no direct evidence is found that such changes in impurity transport take place upon gas injection. In view of robustness of tokamak plasma transport coefficients generally, it seems unlikely that a small gas pulse would change D_z and v_z sufficiently to give the observed impurity behavior. Conjectures have been made in this regard envoking increased edge electrostatic turbulence[21].

6.4 Change in plasma flow pattern in the SOL

When there is no net force the sink action of the SOL on impurity ions would be manifest only through parallel and perpendicular diffusion, to the limiters and to the walls respectively. With small localized limiters and large separation between wall and LCFS, as happens in belt-limiter operation in JET, these diffusive sink mechanisms are weak. Additional sink action in the SOL arises mainly from frictional drag on impurity ions due to plasma flow to the limiters at speed v_{D+}. Measurements of $v_{D+}(y)$, its magnitude and variation with distance y along the SOL, are not available. Models exist for predicting $v_{D+}(y)$ in simple 1-D systems, and sophisticated 1-D and 2-D simulation codes have been used to make forecasts of v_{D+} in the SOL[18], all giving the result that near the limiter $v_{D+} \cong (2kT_e/m_{D+})^{1/2}$ for $T_i=T_e$, but away from the limiter it is much smaller. Lacking verification, a choice from the foregoing models would be arbitrary. Impurities released at the limiter experience strong forces only near the limiter, and different models for v_{D+} would not be expected to give large variations in magnitude of modeled $n_z(0)$. In the present work the purpose is to produce a small effect, a factor $\cong$2 reduction in $n_z(0)$. To find out if reasonable assumptions about $v_{D+}(y)$ could simulate this effect is the object of the exercise, and also to explore whether the experimentally applied changes in gas injection rate could give rise to the necessary changes in $v_{D+}(y)$.

Results in **Tables III-V** were obtained by choosing that $v_{D+}(y)$ and $\tau_{SOL}(y)$ depend linearly on coordinate y, although such simple profiles are not given by any SOL model. A simple fluid model [17,22] assuming a uniform particle source along (y) gives nonlinear relations

$$\mathcal{M}(y) \equiv v_{D+}(y)/c_s = [(y/L)-1]^{-1} + [(y/L-1)^{-2}-1]^{1/2}$$

$$E_{SOL}(y) = \frac{kT_{D+}}{eL} \cdot \frac{\mathcal{M}(1+\mathcal{M}^2)}{(1-\mathcal{M}^2)}$$

L is the connection length and $\mathcal{M}(y)$ and $E_{SOL}(y)$ are respectively the Mach number and the electric field in the SOL. This model may be reasonably realistic for situations without gas injection, where, due to weak deuterium ionization in the SOL, cross- field transport from the core plasma would be the principal particle source for the SOL, with the core plasma being replenished by neutral recycling at the limiters with ionization inside of the LCFS. The principal difference between the linear and the non-linear model, in respect of the frictional force, is that for regions of the SOL away from the limiter the frictional force is weaker in the nonlinear model. Therefore n_z and τ_z would be larger when the nonlinear model of v_{D+} is used in the simulation code. Results are given in **Table VI** showing that $\bar{\tau}_{SOL}$ is indeed larger for the nonlinear model than for the linear one. However, because of the dilution effect of combining $\bar{\lambda}^0_{iz}$ and λ_{SOL}, and because $\lambda_{SOL} \propto (\bar{\tau}_{SOL})^{1/2}$ only, the increase in $n_z(0)$ is small and perhaps indistinguishable from noise in the Monte Carlo calculation.

When gas injection is applied it could, in principle, dominate the particle source in the SOL causing the deuterium plasma to achieve sound speed in the vicinity of the gas source. One might then conjecture that $v_{D+} \cong c_s$ and holding this value for the rest of the SOL. This is surely an extreme assumption, and it will give the strongest credible frictional sink action. Using this constant model with the assumption that $v_{D+}(y)=c_s$ $\bar{\tau}_{SOL}$ was reduced significantly as expected, with a smaller reduction in $n_z(0)$ and $\bar{\tau}_z$, as shown in **Table VI**. Assuming that 'gas off' corresponds to the nonlinear v_{D+} and 'gas on' to the constant v_{D+} models and then simulating the impurity contents gives a reduction of $n_c(0)$ of a factor 2.0/2.5=0.8 and $n_{Be}(0)$ of 1.6/2.8=0.57 respectively for the two gas on/ off comparisons. This matches favorably with the measured ratio of ≅0.7 for carbon and ≅0.5 for beryllium.

In conclusion, it is possible to conjecture changes in the plasma flow pattern along the SOL which would simulate the observed reduction in central impurity density $n_z(0)$. The exercise invokes extreme, barely plausible but not impossible, changes in deuterium plasma flow pattern along the SOL. It is conjectured that gas injection could induce such changes in flow pattern. Verification requires measurements of $v_{D+}(y)$, which have not been made. Proposals to overcome this deficiency have been made[23].

7. Pulses on beryllium limiters with hot spots

Runaway contamination of deuterium plasmas in JET during high power heating is attributed to evaporation of limiter and X-point target tiles (also known as 'bloom' formation), due to overheating of tile edges and formation of hot spots. The concomitant fuel dilution is so large that the DD fusion rate is rapidly reduced to insignificance. The runaway contamination has successfully been arrested by fuel gas injection, so that plasma purity is maintained in spite of hot spots on target plates. In this section we examine the dynamics of plasma contamination when hot spots are formed, first without gas injection. The bare facts of the observations are given in **sec.2** and **Table II**. We think that during heating, in the absence of hot spots, impurity production is mainly due to physical sputtering giving high energy impurity atoms. When hot spots form then, due to evaporation, large quantities of impurities are produced in the form of slow thermal atoms. Sputtered atoms, because of their larger emission energy compared to that of evaporated atoms, penetrate deeper into the plasma, $\bar{\lambda}^0_{iz}(\text{sputtered}) \gg \bar{\lambda}^0_{iz}(\text{thermal})$, giving greater contamination than an equal number of evaporated atoms.

7.1 Contamination efficiency of sputtered and evaporated beryllium atoms

To test this hypothesis LIM simulations of shot #22948 were made. Plasma contamination was calculated with impurity source due to (i) physical sputtering by D+ only, and (ii) physical sputtering by D+ together with self-consistent self-sputtering. This was then compared with that due to the evaporative source wherein a small region on the limiter, 1cm outboard of the LCFS, was taken to be a representative hot spot emitting 0.1eV beryllium atoms with a cosine angular distribution. Calculations were performed of plasma contamination due to (i) thermal (evaporated) impurity source, and (ii) thermal source with beryllium ions returning to

the limiter surface initiating a self-sputtering cascade. Edge electron temperature and density used in the calculations are given in **Table II** and were obtained from other similar shots. Bulk plasma profiles were obtained as usual from interferometry, electron cyclotron emission and Thomson scattering. D_z=0.54m^2/s and v_z= -2D_zr/a^2 together with linear model for $v_{D+}(y)$ and E_{SOL} were assumed. **Table VII** gives the calculated average neutral energy $\mathcal{E}_a$, $\bar{\tau}_{SOL}$, and τ_z.

As expected $\bar{\tau}_{SOL}$ and τ_z are very short when the incident impurity atoms are due to evaporation rather than sputtering. Allowing for effects of self-sputtering, the hot spot case is calculated to have a contamination efficiency smaller than that for the sputtering case, by τ_z/τ_z' = 38/11.5 =3.3, close to the measured efficiency ratio $\langle n_{Be}\rangle/\Phi_{Be}/[\langle n_{Be}\rangle/\Phi_{Be}]'$= 2.5.

Table VII also shows the LIM calculated total sputtering yield Y, for normal ion incidence and allowing for spatial variation of particle flux and temperature in the edge, for beryllium sputtering by deuterium, with and without self-sputtering, giving 0.045 and 0.035 respectively, whereas the measured value is $Y=\Phi_{Be}/\Phi_D=4\times10^{20}/10^{22}=0.04$. Although the measured trends can be simulated many questions remain when absolute magnitudes are compared. Deviations were found as follows:

a. Using **eq.4** and the measured edge data, assuming four limiter surfaces to be wetted by the plasma and that the flux density at the LCFS is given by $n_e(a)c_s(a)$, the deuterium flux was calculated to be $\phi_D \cong 1.4\times10^{23}s^{-1}$, very much larger than the measured flux $\cong10^{22}s^{-1}$. The deduced sputtered beryllium flux ϕ_z^0 is then also an order of magnitude too high.

b. If the measured value of ϕ_z^0 is used together with the code simulation value of τ_z to calculate $\bar{n}_{Be}=\tau_z\phi_z^0/V_p$, then the result is a factor of ≈4 smaller than the measured $\bar{n}_{Be}$. Alternatively, if the code simulation value of ϕ_z^0 is used (sputtering case only) $\bar{n}_{Be}$ is a factor ≈4 too high. It therefore appears that the actual deuterium flux to the limiters is intermediate between that inferred from spectroscopic measurements and that calculated from eq.4. and measured edge data. Other explanations for the discrepancy are possible.

The LIM simulated value of τ_z may be compared with that inferred from eq.3 using calculated values for $\bar{\lambda}^0_{iz}$ and τ_{SOL} (with alteration when $\bar{\lambda}^0_{iz}<0$, as discussed earlier), **Table VII**. Where sputtering is the dominant impurity source, ≈2/3 of beryllium atoms are ionized inboard of the LCFS and the two values of τ_z agree well, confirming the effective uniformity of the influx and outflux. When evaporation dominates agreement between the two values of τ_z is poorer, reflecting the fact that most of the beryllium atoms are ionized in the SOL and that the influx is spatially non-uniform. This change in uniformity of impurity source in going from sputtering to evaporation is indicated also by $\bar{Z}_{Be}$ the average charge of Be ions reaching the limiter, **Table VI**.

7.2 Plasma contamination during hot spots inhibited by gas fueling

In #22957, with identical OH heated target plasma as #22948 previously, fuel gas was injected at 80mbl/s during ICRF heating with P_{ICRF}≅19MW. Although ϕ^0_{Be} increased by more than a factor of ten compared to #22948, runaway beryllium contamination was prevented and the DD fusion rate was sustained for a long time without reduction. Measured densities and fluxes are shown in **Table II**.

As with the earlier studies involving matched discharge pairs, we wish to understand the mechanism giving such a low contamination efficiency in the presence of gas injection. The LIM code was employed with similar assumptions to the last section. $T_e(a)$, $n_e(a)$, λ_T and λ_n, obtained from Langmuir probe measurements, are given in **Table II**. Results of LIM simulations are given in **Table VIII**. For comparison the code was run assuming D+ physical sputtering plus self-sputtering. The value of τ_z is reduced by a factor ≅2 compared with the hot spot case analyzed in **Table VII**, which had no gas injection. Thus the experimental observation that gas injection caused a reduction in hot-spot contamination efficiency by a factor of ≅10 was not reproduced in the LIM simulations. The code was run assuming the constant model for deuterium plasma flow v_{D+} along the SOL, which gives the strongest possible frictional force on the impurities, assuming subsonic plasma flow along B. The result was only a small reduction in τ_z from 5.9ms to 4.7ms.

It thus does not appear to be possible to simulate the strong impurity shielding effect of gas injection for the hot spot discharges, except by invoking some change in cross-field transport near the edge. Transport studies using impurity injection were carried out in these discharges in order to infer impurity transport in the plasma core. No modification of core impurity transport could be associated with fuel gas injection[19]. This still leaves the possibility of changes in the ion transport just at the edge; injection studies of low ionization state impurities will be required to elucidate this question further.

8. Reliability limits

Uncertainty of a factor of two or more is expected in simulation of each step in the link connecting the plasma edge with the impurity content in the plasma core. The experimental values of production rate are based on spectroscopic measurements, requiring conversion of absolute intensities, using theoretical photon efficiencies[24] to infer particle influx rates. Factor of two uncertainty is expected in these efficiencies[24,18]. In addition, the photon efficiency is a strong function of the electron temperature in the emission region. Usually this value of T_e is only estimated. In the case of the shots with hot spots this uncertainty could be particularly large since there is no simple way to establish T_e just at the hot spot. Indeed, it may even be that the most important hot spot is not in the field of view of the spectroscopic instrument[19]. The experimental values of impurity production are therefore in doubt by at least a factor of two.

Production rates can be calculated from Langmuir probe measurements of $n_e(a)$, $T_e(a)$, λ_n, λ_T which are subject to substantial experimental uncertainity, perhaps as large as a factor of two in the case of $n_e(a)$, and laboratory data on sputtering yields. Here too a number of uncertainties arise: (a) are the limiters uniformly loaded on all four plasma-wetted surfaces? (b) should one use the laboratory yield values for normal incidence ions? (c) does $T_i = T_e$ in the SOL? (the ion impact energy is somewhat dependent on T_i) (d) for the hot spots, does the intense impurity production disturb the plasma locally, partially shielding the spot from the plasma heat flux?

Turning to the ion transport it is essential to know D_z and v_z for the impurity species in question, for the discharges being analyzed. Since the coefficients may be radially varying, we need to know them for both the edge $(a-\lambda^{o}_{iz}) \leq r \leq (a+\lambda_{SOL})$, and for the core regions. Moreover the coefficients may be different from those for the fuel species. It is also likely that ion transport is poloidally varying, which would be important for the edge transport where the source and sink action is poloidally localized. Impurity injection experiments aimed at measuring the edge transport should therefore permit poloidal resolution. None of the foregoing transport information is available for the discharges of interest, thereby introducing significant uncertainties in quantitative conclusions from modeling. Fortunately, conclusions of the present study are based largely on comparative rather than absolute impurity densities, mitigating somewhat the effect of uncertainties mentioned above.

9. Summary and conclusions

Experiments in JET have shown that small amount of fuel gas injection during high power heating can substantially reduce central impurity density, without necessarily increasing plasma density or reducing plasma temperatures and fusion rate. How does this reduction in plasma impurity content come about, and is there a distinction between this impurity control effect and the widely observed tokamak behavior that Z_{eff} decreases with increasing $\bar{n}_e$?

Four potential explanations for the impurity control effect were analyzed using the limiter impurity code LIM:

a. reduction in impurity production rate,
b. increase in edge shielding due to more superficial ionization,
c. increase in radial transport, in the bulk and/or edge plasma,
d. increase in flow in the SOL plasma.

Pairs of JET shots, with/without fuel gas injection, for both carbon and beryllium limiter configurations, were analyzed. A valuable simplifying factor characterizing these shots was that due to beryllium gettering a single impurity was dominant and oxygen was negligible. The LIM code simulation, assuming physical sputtering only, showed that impurity production actually increased when the fuel gas pulse was applied, ruling out (a) as a possible explanation. Increase in edge shielding, although

in the desired direction, was too small in magnitude to explain the observed impurity reduction, thus ruling out (b). Increase in radial impurity transport could readily explain the observed reduction, a factor of two increase in D_z in only a narrow region at the edge would be sufficient. Changes in D_z at the edge have not been measured, but measurements have ruled out such changes in D_z in the bulk plasma. Hypothesized changes in deuterium plasma flow pattern along the SOL, if pushed to extremes, could produce the observed reduction in core impurity density; again confirmation of such changes in flow pattern is lacking.

When high power heating was applied in beryllium limiter configuration, runaway beryllium contamination of the deuterium plasmas was observed due to formation of hot spots on the limiters and eventual melting, which was determined in postmortem analysis of limiter tiles. Large increase in beryllium influx was observed spectroscopically, which then quenched the DD fusion reaction rate. Fuel gas injection during heating was able to prevent runaway contamination and loss of fusion reactivity, although the beryllium impurity production rate even increased. For medium heating power of ≅10MW and in the absence of gas injection, LIM code analysis showed that the reduced contamination efficiency of impurities could be understood by the small energy of neutrals from hot spots(0.1 eV) in comparison to that of sputtered ones(10 eV). The evaporated neutrals penetrate the plasma less before ionizing and are thus better shielded from reaching the core plasma. Using strong fuel gas injection to inhibit contamination during ≅20MW heating, the low contamination efficiency could not be explained without invoking increases in radial impurity ion transport or average flow velocity.

Thus the observed strong impurity shielding produced by injection of a small amount of fuel gas, in the presence of much larger recycling flux, can be simulated only by invoking increase in radial impurity transport at the edge, and/or changes in parallel transport due to increase in deuteron flow in the SOL. Direct experimental refutation of these is lacking, but there is indirect evidence that increase in edge transport may be excluded. The required average flow velocity for the latter to be effective is implausibly large. Thus, in order to be able to describe the experimental observations, it may be necessary to postulate additions to the processes already considered in the reference model.

10. Acknowledgements

The authors are grateful to S.K.Erents, P.D.Morgan, D.Pasini, M.F.Stamp and M.von Hellermann for making edge plasma and impurity measurements and making data available. P.C.Stangeby and J.D.Elder acknowledge support by the Canadian Fusion Fuels Technology Project.

11. References

[1] A.Gondhalekar et al, Journal of Nuclear Materials. 176&177(1990)600.

[2] P.D.Morgan et al., Europhysics Conference Abstracts. 11D-III(1987)1240.

[3] A.Boileau et al., Nuclear Fusion 29(1989)1449.

[4] W.Engelhardt and W.Feneberg, Journal of Nucl. Mater. 76&77(1978)518.

[5] P.C.Stangeby, Journal of Nuclear Materials 176&177(1990)51.

[6] P.C.Stangeby, Contributions to Plasma Physics 28(1988)507.

[7] J.N.Brooks et al., Contributions to Plasma Physics 28(1988)465.

[8] S.Sengoku and H.Ohtsuka, Journal of Nuclear Materials 93&94(1980)75.

[9] M.W.Thompson, Philosophical Magazine 18(1968)377.

[10] J.Bohdansky, Special Issue of Nuclear Fusion (1984)61.

[11] J.Roth, Max-Planck Institut für Plasmaphysik, private communication 1989, The sputtering constants used, E_{th}(eV)|E_{TF}(eV)|Q, are as follows: (i) D on C: 28|446|0.14; (ii) C on C: 42|5680|1.3; (iii) D on Be: 10|280|0.27; (iv) Be on Be: 35|2210|0.94.

[12] J.Roth, in: Physics of Plasma-Wall Interactions in Controlled Fusion, Eds. D.E Post and R.Behrisch, Plenum Press, New York, 1986, p351.

[13] A.A.Haasz et al, Journal of Nuclear Materials 162-164(1989)915.

[14] D.E.Post and K.Lackner, in: Physics of Plasma-Wall Interactions in Controlled Fusion, Eds. D.E Post and R.Behrisch, Plenum Press, New York, 1986, p627.

[15] P.C.Stangeby, Journal of Nuclear Materials 145-147(1987)105.

[16] A.Gondhalekar et al., Plasma Physics and Controlled Fusion 31(1989)805.

[17] S.A.Self and H.N.Ewald, Phys. Fluids 9(1966)2486.

[18] P.C.Stangeby and G.M.McCracken, Nuclear Fusion 30(1990)1225.

[19] A.Gondhalekar et al.,Europhysics Conference Abstracts, 15C-I(1991)25.

[20] D.Hildebrandt, Contributions to Plasma Physics 26(1986)231.

[21] N.L.Vasin et al., Europhysics Conference Abstracts 12B-I(1988)59.

[22] P.C.Stangeby et al.,Nuclear Fusion 28(1988)1945.

[23] P.C.Stangeby and J.D.Elder, Plasma Phys. and Contr. Fusion 33(1991)1435.

[24] K.Behringer et al, Plasma Physics and Controlled Fusion 31(1989)2059.

TABLE I

Summary of electron and impurity densities at the plasma center, electron density and temperature at the LCFS and corresponding thicknesses of the SOL, for two pairs of nearly identical JET shots. One shot in each pair employed a gas pulse to inhibit impurity contamination.

JET Shot #	19643	19648	20674	20675
Time	9.5s	9.5s	11s	11s
D_2 fuel gas pulse	OFF	57 mbl/s	OFF	100 mbl/s
Limiter material and main impurity	C	C	Be	Be
P_{ADD}	14 MW		16 MW	
$n_e(0)$ $[10^{19}m^{-3}]$	5.7	6.0	5.0	5.2
$n_Z(0)$ $[10^{18}m^{-3}]$ VB	5.6	3.8	3.6	1.7
$n_Z(0)$ $[10^{18}m^{-3}]$ SXR	4.7	3.3	-	-
$n_Z(0)$ $[10^{18}m^{-3}]$ CXRS	6.7	4.7	4.5	2.3
$n_e(a)$ $[10^{18}m^{-3}]$	7.8	17.7	4	6.7
$T_e(a)$ [eV]	52	52	35	28
λ_n [mm]	15	11	10	9
λ_T [mm]	27	19	23	25

TABLE II

Summary of shots on beryllium belt limiter, with high power heating, whereby hot spots formed on the limiter. Comparison is shown between plasmas without and with hot spots, and a shot with a hot spot where gas injection was employed to inhibit runaway beryllium contamination.

JET Shot #	22948		22957
D_2 gas pulse	NO	NO	80 mbl/s
Limiter material and main impurity	Be	Be	Be
P_{ADD}(MW)	0	10	19
Hot spots?	NO	YES	YES
$\langle n_e \rangle$ [$10^{19} m^{-3}$]	1.6	2	4
$\langle n_D \rangle$ [$10^{19} m^{-3}$]	1.3	1.2	3.4
$\langle n_{Be} \rangle$ [$10^{19} m^{-3}$]	0.05	0.15	0.2
$T_e(0)$ [keV]		9	9
$T_i(0)$ [keV]		5.5	4
Φ_D [10^{20} atoms/s]	100	100	250
Φ_{Be} [10^{20} atoms/s]	4	30	>300
Z_{eff}	1.5	2.4	2.4
$n_e(a)$ [$10^{18} m^{-3}$]		7	8
$T_e(a)$ [eV]		100	66
λ_n [mm]		8.2	8.7
λ_T [mm]		33.1	17

TABLE III

LIM code simulations of impurity production, impurity confinement time, and central impurity density, together with additional output on the average distance inboard of the LCFS where ionization occurs $\bar{\lambda}^0_{iz}$, the average impurity dwell time in the SOL $\bar{\tau}_{SOL}$, and the radial length scale for impurity density decay λ_{SOL}. Measured SOL parameters of Table I were used in the calculations.

JET Shot #	19643	19648	20674	20675
D_2 fuel gas pulse	OFF	ON	OFF	ON
Main impurity	C	C	Be	Be
Total impurity production ϕ^0_z [10^{21}/s]	6.1	9.8	4.2	5.6
$\bar{\lambda}^0_{iz}$ [mm], average ionization depth	3.6	1.1	6.5	2.1
$\bar{\tau}_{SOL}$ [ms], average dwell time in SOL	0.25	0.18	0.51	0.3
$\lambda_{SOL} = (D_{\perp z}\bar{\tau}_{SOL})^{1/2}$ [mm]	12	9.9	17	13
$\bar{Z}_{lim}$ the average charge of ions striking the limiters	3.39	3.06	2.68	2.44
Impurity confinement time τ_z [ms]	33	22	43	27
Impurity density $n_z(0)$ [$10^{18}/m^3$]	2.4	2.5	2.4	1.9

TABLE IV

LIM code simulation of primary impurity production by sputtering, and the energy and ionization of these. Also tabulated is production of secondary impurities by self consistent self-sputtering, energy and ionization of these. Measured SOL parameters of Table I were used in the calculations.

JET Shot #	19643	19648	20674	20675
D_2 fuel gas pulse	OFF	ON	OFF	ON
Main impurity	C	C	Be	Be
Average energy [eV] of neutrals due to D^+ sputtering, (primary impurities)	11	11	6	5.4
Fraction of primary impurities ionized inside LCFS	0.62	0.51	0.78	0.72
Average energy [eV] of neutrals due to self-sputtering, (secondary impurities)	36	35	16	16
Fraction of secondary impurities ionized inside LCFS	0.72	0.64	0.79	0.77
Primary sputtering yield	0.026	0.025	0.068	0.065
Total sputtering yield, Y_{tot}	0.034	0.033	0.079	0.074
Total deuteron flux to limiters $\phi_{D+}[10^{23}/s]$	1.8	3.0	0.53	0.76
Total impurity production rate $\phi_Z^0 = Y_{tot} \cdot \phi_{D+}$ $[10^{21}/s]$	6.1	9.8	4.2	5.6

TABLE V

Comparison between $n_z(0)$ and τ_z calculated directly by the LIM code and that deduced from analytic expressions using subsidiary LIM code output of $\bar{\lambda}^0_{iz}$ and λ_{SOL}.

JET Shot #	19643	19648	20674	20675
D_2 fuel gas pulse	OFF	ON	OFF	ON
Main impurity	C	C	Be	Be
$n_z(0)$ [$10^{18}m^{-3}$] directly calculated by LIM code	2.4	2.5	2.4	1.9
$n_z(0)$ [$10^{18}m^{-3}$] calculated using eq.1 with code calculated $\bar{\lambda}^0_{iz}$ and λ_{SOL}	2.7	3.1	2.9	2.4
τ_z [ms] directly calculated by code	33	22	43	27
τ_z [ms] calculated using eq.3 with code calculated $\bar{\lambda}^0_{iz}$ and λ_{SOL}	33	23	49	32
$\bar{n}_z V_p / \phi^0_z \tau_z$	0.83	0.80	0.92	0.87

TABLE VI

LIM code simulations of effects of assuming different models for flow in the SOL on central impurity density $n_z(0)$, average impurity confinement time $\bar{\tau}_z$, average impurity dwell time in the SOL $\bar{\tau}_{SOL}$.

JET Shot #	19643	19648	20674	20675
D_2 fuel gas pulse	OFF	ON	OFF	ON
Main impurity	C	C	Be	Be
$n_z(0)$ [$10^{18} m^{-3}$], linear model	2.4	2.5	2.4	1.9
$n_z(0)$ [$10^{18} m^{-3}$], nonlinear model	2.5		2.8	
$n_z(0)$ [$10^{18} m^{-3}$], constant model		2.0		1.6
$\bar{\tau}_z$ [ms], linear model	33	22	43	27
$\bar{\tau}_z$ [ms], nonlinear model	32		53	
$\bar{\tau}_z$ [ms], constant model		18		22
$\bar{\tau}_{SOL}$ [ms], linear model	0.25	0.18	0.51	0.30
$\bar{\tau}_{SOL}$ [ms], nonlinear model	0.44		0.82	
$\bar{\tau}_{SOL}$ [ms], constant model		0.073		0.14

Table VII

LIM code simulation of Be-limiter shot # 22948, in which rapid runaway contamination of the plasma took place due to formation of a hot spot. Tabulation compares contamination efficiency of sputtered and evaporated beryllium impurity.

Measured $T_e(a)$=100eV, $n_e(a)=7\times10^{18}m^{-3}$, λ_T=33.1mm, λ_n=8.2mm

A D^+ Physical sputtering only

B D^+ Sputtering plus self-sputtering

C Evaporation only

D Evaporation plus self-sputtering

	A	B	C	D
Average neutral beryllium atom energy $\mathcal{E}_a$ [eV]	10.5	13.2	0.1	3.2
Fraction of Total Release due to self-sputtering		0.23		0.19
$\bar{\tau}_{SOL}$ [ms]	0.22	0.24	0.044	0.073
τ_z [ms]	33	38	4.6	11.5
$\bar{\lambda}^0_{iz}$ [mm]	+4.2	+4.3	-7.1	-4.9
Fraction of beryllium atom ionized inside LCFS	0.66	0.65	0.021	0.14
Total sputtering yield	0.035	0.045		
τ_z calculated from $\bar{\lambda}^0_{iz}$ and τ_{SOL} [ms]	33	35	2.5	6.5
Average value of Z of Be flux to limiters	2.7	2.7	1.6	1.8

Table VIII

LIM code simulation of Be-limiter shot #22957, where a gas pulse was used during high power heating to inhibit runaway contamination due to formation of hot spots.

Measured $T_e(a)=66eV$, $n_e(a)=8x10^{18}m^{-3}$, $\lambda_T=17mm$, $\lambda_n=8.7mm$

	D^+ sputtering plus self-sputtering	Evaporation plus self-sputtering
Average energy of Be atom [eV]	10.1	1.7
Fractional total release due to self-sputtering	0.19	0.10
$\bar{\tau}_{SOL}$ [ms]	0.36	0.091
τ_z [ms]	34	5.9
Fraction of beryllium atoms ionized inside the LCFS	0.68	0.097
Average value of Z of Be flux to limiters	2.6	1.7

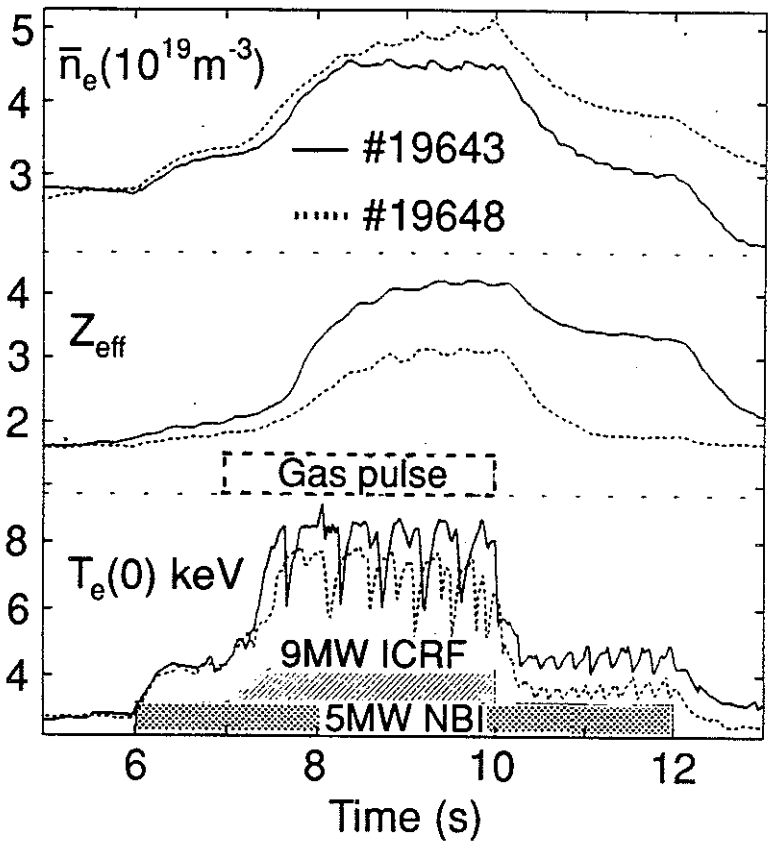

Fig.1 Comparison of evolution of $\bar{n}_e$, Z_{eff} and $T_e(0)$ during high power NBI and ICRF heating, showing the ability to reduce Z_{eff} of the plasma without much increasing $\bar{n}_e$ or decreasing $T_e(0)$, by fuel gas injection during high power heating, for beryllium gettered belt carbon limiter operation.

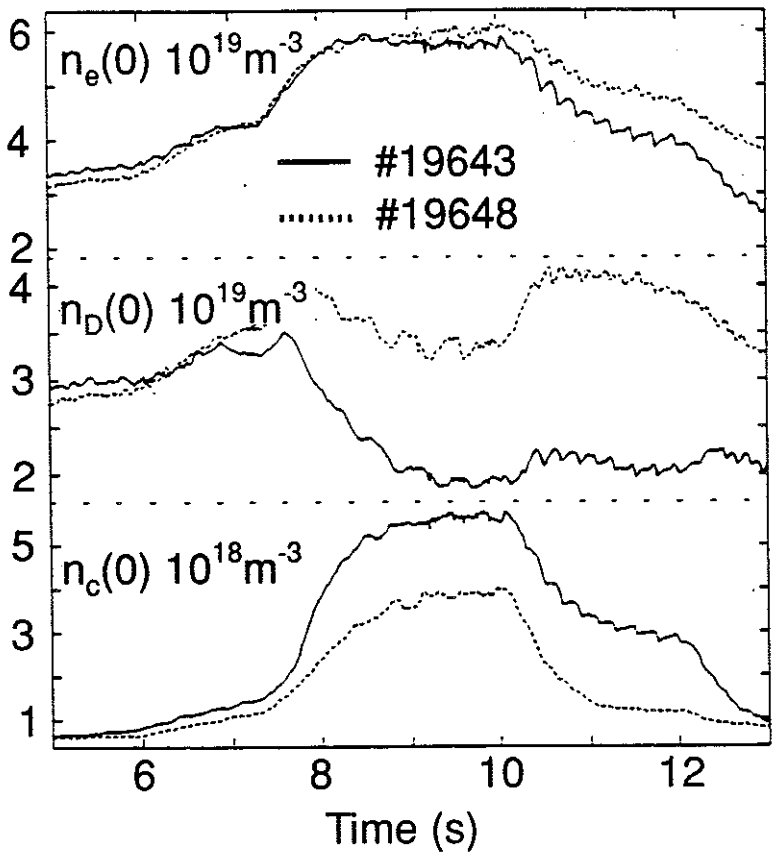

Fig.2 Comparison of evolution of peak electron, deuteron, and carbon densities, $n_e(0)$, $n_D(0)$ and $n_C(0)$, during high power heating, showing the impurity shielding effect of fuel gas injection,for operation on beryllium gettered carbon belt limiters.

Appendix I

THE JET TEAM

JET Joint Undertaking, Abingdon, Oxon, OX14 3EA, U.K.

J.M. Adams[1], B. Alper, H. Altmann, A. Andersen[14], P. Andrew, S.Ali-Arshad, W. Bailey, B. Balet, P. Barabaschi, Y. Baranov, P. Barker, R. Barnsley[2], M. Baronian, D.V. Bartlett, A.C. Bell, G. Benali, P. Bertoldi, E. Bertolini, V. Bhatnagar, A.J. Bickley, D. Bond, T. Bonicelli, S.J. Booth, G. Bosia, M. Botman, D. Boucher, P. Boucquey, M. Brandon, P. Breger, H. Brelen, W.J. Brewerton, H. Brinkschulte, T. Brown, M. Brusati, T. Budd, M. Bures, P. Burton, T. Businaro, P. Butcher, H. Buttgereit, C. Caldwell-Nichols, D.J. Campbell, D. Campling, P. Card, G. Celentano, C.D. Challis, A.V.Chankin[23], A. Cherubini, D. Chiron, J. Christiansen, P. Chuilon, R. Claesen, S. Clement, E. Clipsham, J.P. Coad, I.H. Coffey[24], A. Colton, M. Comiskey[4], S. Conroy, M. Cooke, S. Cooper, J.G. Cordey, W. Core, G. Corrigan, S. Corti, A.E. Costley, G. Cottrell, M. Cox[7], P. Crawley, O. Da Costa, N. Davies, S.J. Davies[7], H. de Blank, H. de Esch, L. de Kock, E. Deksnis, N. Deliyanakus, G.B. Denne-Hinnov, G. Deschamps, W.J. Dickson[19], K.J. Dietz, A. Dines, S.L. Dmitrenko, M. Dmitrieva[25], J. Dobbing, N. Dolgetta, S.E. Dorling, P.G. Doyle, D.F. Düchs, H. Duquenoy, A. Edwards, J. Ehrenberg, A. Ekedahl, T. Elevant[11], S.K. Erents[7], L.G. Eriksson, H. Fajemirokun[12], H. Falter, J. Freiling[15], C. Froger, P. Froissard, K. Fullard, M. Gadeberg, A. Galetsas, L. Galbiati, D. Gambier, M. Garribba, P. Gaze, R. Giannella, A. Gibson, R.D. Gill, A. Girard, A. Gondhalekar, D. Goodall[7], C. Gormezano, N.A. Gottardi, C. Gowers, B.J. Green, R. Haange, A. Haigh, C.J. Hancock, P.J. Harbour, N.C. Hawkes[7], N.P. Hawkes[1], P. Haynes[7], J.L. Hemmerich, T. Hender[7], J. Hoekzema, L. Horton, J. How, P.J. Howarth[5], M. Huart, T.P. Hughes[4], M. Huguet, F. Hurd, K. Ida[18], B. Ingram, M. Irving, J. Jacquinot, H. Jaeckel, J.F. Jaeger, G. Janeschitz, Z. Jankowicz[22], O.N. Jarvis, F. Jensen, E.M. Jones, L.P.D.F. Jones, T.T.C. Jones, J-F. Junger, F. Junique, A. Kaye, B.E. Keen, M. Keilhacker, W. Kerner, N.J. Kidd, R. Konig, A. Konstantellos, P. Kupschus, R. Lässer, J.R. Last, B. Laundy, L. Lauro-Taroni, K. Lawson[7], M. Lennholm, J.Lingertat[13], R.N. Litunovski, A. Loarte, R. Lobel, P. Lomas, M. Loughlin, C. Lowry, A.C. Maas[15], B. Macklin, C.F. Maggi[16], G. Magyar, V. Marchese, F. Marcus, J. Mart, D. Martin, E. Martin, R. Martin-Solis[8], P. Massmann, G. Matthews, H. McBryan, G. McCracken[7], P. Meriguet, P. Miele, S.F. Mills, P. Millward, E. Minardi[16], R. Mohanti[17], P.L. Mondino, A. Montvai[3], P. Morgan, H. Morsi, G. Murphy, F. Nave[27], S. Neudatchin[23], G. Newbert, M. Newman, P. Nielsen, P. Noll, W. Obert, D. O'Brien, J. O'Rourke, R. Ostrom, M. Ottaviani, S. Papastergiou, D. Pasini, B. Patel, A. Peacock, N. Peacock[7], R.J.M. Pearce, D. Pearson[12], J.F. Peng[26], R. Pepe de Silva, G. Perinic, C. Perry, M.A. Pick, J. Plancoulaine, J-P. Poffé, R. Pohlchen, F. Porcelli, L. Porte[19], R. Prentice, S. Puppin, S. Putvinskii[23], G. Radford[9], T. Raimondi, M.C. Ramos de Andrade, M. Rapisarda[29], P-H. Rebut, R. Reichle, S. Richards, E. Righi, F. Rimini, A. Rolfe, R.T. Ross, L. Rossi, R. Russ, H.C. Sack, G. Sadler, G. Saibene, J.L. Salanave, G. Sanazzaro, A. Santagiustina, R. Sartori, C. Sborchia, P. Schild, M. Schmid, G. Schmidt[6], H. Schroepf, B. Schunke, S.M. Scott, A. Sibley, R. Simonini, A.C.C. Sips, P. Smeulders, R. Smith, M. Stamp, P. Stangeby[20], D.F. Start, C.A. Steed, D. Stork, P.E. Stott, P. Stubberfield, D. Summers, H. Summers[19], L. Svensson, J.A. Tagle[21], A. Tanga, A. Taroni, C. Terella, A. Tesini, P.R. Thomas, E. Thompson, K. Thomsen, P. Trevalion, B. Tubbing, F. Tibone, H. van der Beken, G. Vlases, M. von Hellermann, T. Wade, C. Walker, D. Ward, M.L. Watkins, M.J. Watson, S. Weber[10], J. Wesson, T.J. Wijnands, J. Wilks, D. Wilson, T. Winkel, R. Wolf, D. Wong, C. Woodward, M. Wykes, I.D. Young, L. Zannelli, A. Zolfaghari[28], G. Zullo, W. Zwingmann.

PERMANENT ADDRESSES

1. UKAEA, Harwell, Didcot, Oxon, UK.
2. University of Leicester, Leicester, UK.
3. Central Research Institute for Physics, Budapest, Hungary.
4. University of Essex, Colchester, UK.
5. University of Birmingham, Birmingham, UK.
6. Princeton Plasma Physics Laboratory, New Jersey, USA.
7. UKAEA Culham Laboratory, Abingdon, Oxon, UK.
8. Universidad Complutense de Madrid, Spain.
9. Institute of Mathematics, University of Oxford, UK.
10. Freien Universität, Berlin, F.R.G.
11. Royal Institute of Technology, Stockholm, Sweden.
12. Imperial College, University of London, UK.
13. Max Planck Institut für Plasmaphysik, Garching, FRG.
14. Risø National Laboratory, Denmark.
15. FOM Instituut voor Plasmafysica, Nieuwegein, The Netherlands.
16. Dipartimento di Fisica, University of Milan, Milano, Italy.
17. North Carolina State University, Raleigh, NC, USA
18. National Institute for Fusion Science, Nagoya, Japan.
19. University of Strathclyde, 107 Rottenrow, Glasgow, UK.
20. Institute for Aerospace Studies, University of Toronto, Ontario, Canada.
21. CIEMAT, Madrid, Spain.
22. Institute for Nuclear Studies, Otwock-Swierk, Poland.
23. Kurchatov Institute of Atomic Energy, Moscow, USSR
24. Queens University, Belfast, UK.
25. Keldysh Institute of Applied Mathematics, Moscow, USSR.
26. Institute of Plasma Physics, Academica Sinica, Hefei, P. R. China.
27. LNETI, Savacem, Portugal.
28. Plasma Fusion Center, M.I.T., Boston, USA.
29. ENEA, Frascati, Italy.

At 1st July, 1992